ACTA IMEKO
ISSN: 2221-870X
December 2025, Volume 14, Number 4, 1 - 6

Operating principle of an electric current primary standard based on Ohm's law, the Josephson and the quantum Hall effects

Regis P. Landim[1], Wesley C. S. Sousa[2]

[1] *Instituto Nacional de Metrologia, Qualidade e Tecnologia, Nossa Sra. das Graças 50, 25250-020 Duque de Caxias, Brazil*
[2] *Marinha do Brasil, Grupo Aeronaval de Manutenção, Rua Comandante Ituriel SN, 28944-054 São Pedro da Aldeia, Brazil*

ABSTRACT
Ammeters in the range from nanoamperes to milliamperes are widely used in fundamental and applied metrology, industry, microelectronics, medical care, and healthcare. The calibration of these instruments needs calibration standards to provide a minimum quality process and traceability, which are essential for measurement systems. In Brazil, there is no DC current primary standard. In this ongoing work, we are developing an electric current primary standard based on Ohm's law in the range from nanoamperes to milliamperes. Such a system, based on Ohm's law, is one of the BIPM recommendations to realize the ampere. In this paper, we show the most important phenomena present in electric current standards based on Ohm's law, obtained through the integration of a standard resistor, directly calibrated using a quantum Hall system, and a Josephson voltage standard. Additionally, this article presents the results of the software developed so far, in Python, to integrate the system's components. Using the proposed system, we performed calibrations of a 5730A Fluke calibrator, working as a DC current source, in the range of 50 µA to 10 mA. The obtained uncertainties ranged between 0.5 µA/A and 4.6 µA/A, comparable to the best ones in the Calibration and Measurement Capabilities (CMC) acknowledged by the International Bureau of Weights and Measures (BIPM).

Section: RESEARCH PAPER

Keywords: current primary standard; Josephson voltage standard; quantum Hall system

Citation: R. P. Landim, W. C. S. Sousa, Operating principle of an electric current primary standard based on Ohm's law, the Josephson and the quantum Hall effects, Acta IMEKO, vol. 14 (2025) no. 4, pp. 1-6. DOI: 10.21014/actaimeko.v14i4.1993

Section Editor: Carlos Hall, PósMQI/PUC-Rio, Rio de Janeiro, Brazil

Received November 27, 2024; **In final form** October 26, 2025; **Published** December 2025

Corresponding author: Regis P. Landim, e-mail: rplandim@inmetro.gov.br

1. INTRODUCTION

Electrical current meters are widely used in fundamental and applied metrology, in the semiconductor industry, and in healthcare (dosimeters) [1], as well as in the energy market. With the widespread popularity of smart energy meters, a large amount of electricity data is collected, such as energy consumption, voltage, and current data [2]. The calibration of these meters requires calibration standards traceable to the ampere SI unit.

For the calibration of current meters, the International Bureau of Weights and Measures (BIPM) established in 2019 three ways to do the practical realization of the ampere: (a) by using Ohm's law, the unit relation A = V/Ω, from practical realizations of voltage and resistance; (b) by using a single electron transport (SET), the unit relation A = C/s; and (c) by using the ratio $I = C\,\mathrm{d}V/\mathrm{d}t$, the unit relation A = F·V/s, which corresponds to the current flowing in a capacitor of capacitance C submitted to a voltage ramp over time. Worth mentioning that at the 26th General Conference on Weights and Measures (CGPM), held in 2018, there was a redefinition of the SI in which, among other decisions, it was established that a unit can be realized by any convenient equation of physics that links the defining constants to the quantity intended to be measured [3].

Brazil still lacks an electric current primary standard. In this article, we present the preliminary results of an electric current primary standard based on Ohm's law, which integrates the primary standards of voltage and electrical resistance (obtained from the Josephson and the quantum Hall effects, respectively).

In Section 2, we explain the concepts of the Josephson and the quantum Hall effects, as well as the PJVS (Programmable Josephson Voltage Standard) and the quantum Hall systems that implement these effects. In Section 3, we present the proposed system. In Section 4, we make a brief uncertainty analysis. In

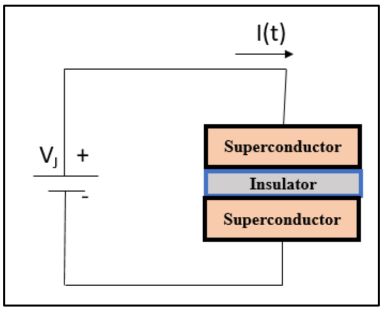

Figure 1. Josephson Junction representation.

Section 5, we present some experimental results, analysis, and the validity of this proposal. In Section 6, there are the conclusions of the work done so far in this research.

2. THE JOSEPHSON EFFECT, THE QUANTUM HALL EFFECT, AND THE SYSTEMS THAT IMPLEMENT THEM

The Josephson effect, discovered in 1962 by the physicist Brian David Josephson, consists of the observation of the following phenomenon: a junction, composed of two superconductors separated by a thin insulating material, named Josephson Junction (JJ), will have a current $I(t)$ flowing between the two superconductors through the insulator, as shown in Figure 1 (the insulator layer is out of scale) [4].

This happens even when there is no application of an electric potential ($V_{\mathrm{J}} = 0$) between the superconductors; therefore, this current is not related to Ohm's law. In this case, Cooper pairs (via the quantum tunnelling effect) compose what is called the "critical current", which exists in both directions [5]. This observation is called the Josephson DC effect, and the critical current for zero JJ voltage is shown in Figure 2, where, for $V_{\mathrm{J}} = 0$, it is observed that the current I, presented on the ordinate axis, reaches the same value in both sides (200 µA).

Additionally, if (in the same structure shown in Figure 1) a voltage VJ is applied between the superconductors, a current with a well-defined frequency is observed, which depends on the potential difference VJ applied. This effect, called the AC Josephson effect, occurs due to the same phenomena as described in the Josephson DC effect (Cooper pairs and quantum tunnelling) [6].

Thus, due to the AC Josephson effect, one can establish a direct relationship between the voltage at the leads of a JJ and the frequency of the current flowing through the JJ's insulator, as defined by equations (1) and (2). Therefore, when crossing a JJ with a current of frequency f, a voltage VJ that is obtained, in

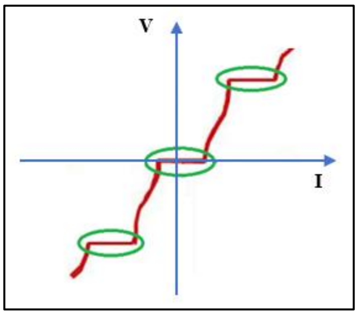

Figure 3. Voltage steps between the subarray leads, due to microwave frequency around 20 GHz (NIST design). They are activated by bias current (I).

this context, depends only on the frequency of the current applied to the JJ and its associated uncertainty [6], [7].

$$V_{\mathrm{J}} = \frac{h}{2.e} f = \frac{f}{K_{\mathrm{J}}} \tag{1}$$

$$K_{\mathrm{J}} = \frac{2 \cdot e}{h} = 483\,597\,848.416\,984\ \mathrm{GHz/V}\,, \tag{2}$$

where f is the frequency of the current flowing through the junction; K_{J} is the Josephson constant [3]; e is the elementary charge, given by $1.602\ 176\ 634 \times 10^{-19}$ C [3]; h is Planck's constant, given by $6.626\ 070\ 15 \times 10^{-34}$ J s [3]; V_{J} is the voltage applied across the terminals of the Josephson junction; all quantities are in SI units, unless stated differently.

The Josephson effect is used in primary voltage standard systems (the details of which are beyond the scope of this paper), such as the Programmable Josephson Voltage Standard (PJVS) [6], [7]. Basically, this system receives a frequency signal, around 75 GHz (Physikalisch-Technische Bundesanstalt – PTB-design) or 20 GHz (National Institute of Standards and Technology – NIST-design), which reaches a group of JJs, called a subarray, which (in its turn) will induce the current I, that will flow through the JJ. As previously described in relation to the AC Josephson effect, because of this current through the junction, step voltage values V_{J} will be established between the leads of a group of JJs, in certain regions, which remain constant for small variations in polarization current (I), as shown in Figure 3 (in green).

It is possible to apply a bias current to a group of JJs, allowing the activation of either the negative step or the positive one, for this group of JJs. Therefore, it is possible to control and mathematically determine, through equations (1) and (2), the Josephson voltage value V_{J} [6]. The Josephson voltage value V_{J},

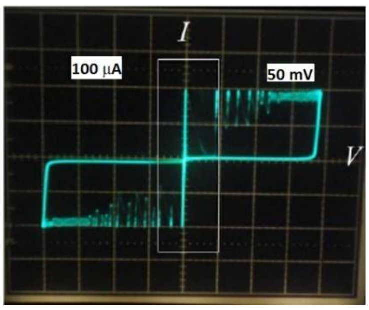

Figure 2. The current I that flows through a conventional Josephson Junction as a function of V_{J}. Oscilloscope adjusted to 50 mv/div. horizontal and 100 µA/div. vertical.

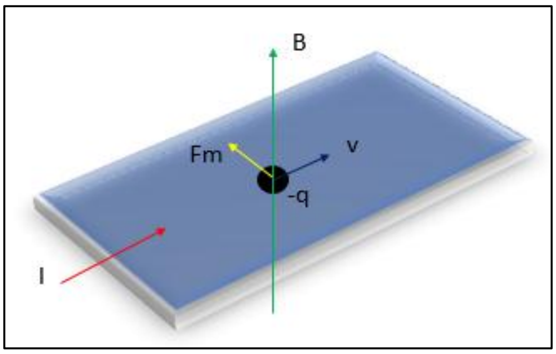

Figure 4. Magnetic force $\vec{F}_m$ acting on a charge -q with velocity $\vec{v}$.

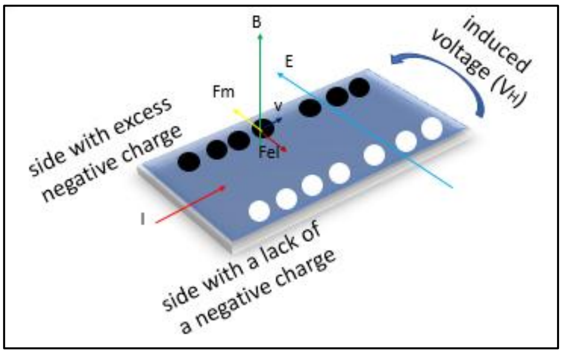

Figure 5. Magnetic force $\vec{F}_m$ acting on a charge $-q$ with velocity $\vec{v}$.

resulting from the association of one or more JJ groups, allows calibrating an external voltage standard through a null detector.

The Hall effect is observed in a conducting plate, subjected to a current I and a magnetic field $\vec{B}$ perpendicular to this current. This will provide an induced magnetic force, $\vec{F}_m$, due to the interaction between the charge velocity $-q$ and the magnetic field $\vec{B}$, given by equation (3). One can see a representation of this phenomenon in Figure 4:

$$\vec{F}_m = q \cdot \vec{v} \times \vec{B}\,, \tag{3}$$

where $\vec{F}_m$ is the magnetic force, in N; q is the charge value, in C; $\vec{v}$ is the speed of the charge, in m/s; $\vec{B}$ is the magnetic flux density, in T.

Due to the magnetic force, the charges will concentrate on one side of the plate. This concentration creates a voltage V_{H} and an electric field $\vec{E}$ between each side of the plate (parallel to the velocity $\vec{v}$). The interaction of the electric field $\vec{E}$ with the charge creates an electric force $\vec{F}_{el}$ that acts on the charge, until it balances with the magnetic force $\vec{F}_m$. Figure 5 shows the phenomenon described, called the Hall effect.

According to Ohm's law, the relationship between the longitudinal electrical voltage (V_{L}) that generates the current I and this same current defines the longitudinal resistance, presented in equation (4), and the relationship between the electrical voltage originating from the electric field E (V_{H}) and the current I defines the Hall resistance R_{H}, presented in equation (5) [8]:

$$R_{\mathrm{L}} = \frac{V_{\mathrm{L}}}{I} \tag{4}$$

$$R_{\mathrm{H}} = \frac{V_{\mathrm{H}}}{I}\,. \tag{5}$$

The quantum Hall effect occurs at temperatures below 0.3 K, where quantum phenomena are observed; the curve of these resistances, as a function of the magnetic field $\vec{B}$, is shown in Figure 6 (b).

In 1980, K. Von Klitzing subjected the SI-MOSFET material to magnetic fields above 19.8 T and temperatures below 4.2 K. Thus, he determined the fundamental von Klitzing constant, R_{K} [9]. This constant depends on the elementary charge e and Planck's constant h, according to equation (6) [10]:

$$R_{\mathrm{K}} = \frac{h}{e^2} = 25\,812.807\,459\,3045\;\Omega\,, \tag{6}$$

where the value of the von Klitzing constant R_{K} is given inequation [11]; h is given by 6.626 070 15 × 10^{-34} J s [3], and e is given by 1.602 176 634 × 10^{-19} C [3].

The resistance R_{H} can be expressed as a function of the constant R_{K} according to equation (7) [9]:

$$R_{\mathrm{H}} = \frac{R_{\mathrm{K}}}{i}\,, \tag{7}$$

where i is an integer number, and therefore R_{H} takes only values that are multiples of R_{K}. The i value represents the plateau of the magnetic field in the curve shown in Figure 6 (b).

In this way, the resistance standard is obtained by subjecting a semiconductor material (generally the GaAs and AlGaAs junction) to an intense magnetic field at temperatures below 4 K, as shown in Figure 6 (a).

Thus, when varying the magnetic field, the resistance value R_{H} (function of V_{H}) and resistance R_{L} (function of V_{XX}) are as shown in Figure 6 (b). The standard resistance value is then obtained from the identification of the plateau of the curve shown in Figure 6 (b) (i value) and dividing the R_{K}constant by the identified i [9].

According to Figure 7, typical 100 Ω standard R_{S} resistors are calibrated by comparing them with the calculated value of R_{H}, given by equation (7). The primary resistance standard system

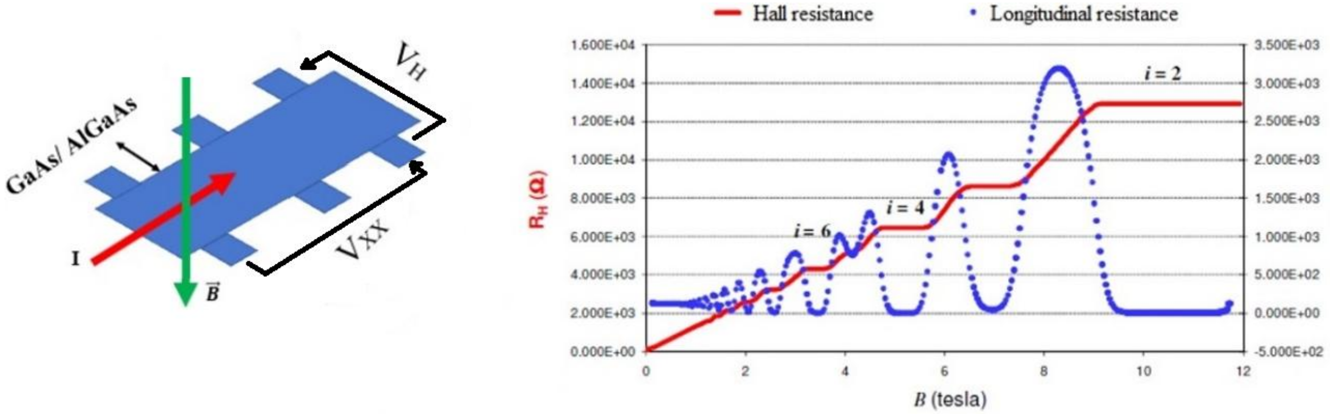

(a) (b)

Figure 6. Representation of the electrical resistance curves as a function of the magnetic field: a) working principle of the resistance standard, b) resistances as functions of the magnetic field.

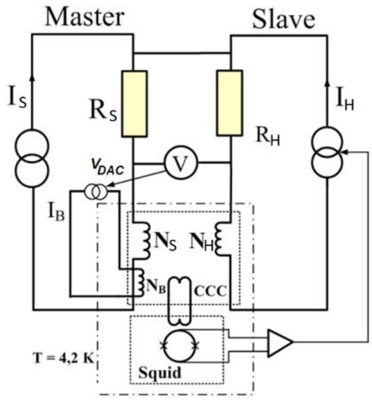

Figure 7. QHS CCC representation.

(the details of which are beyond the scope of this paper), known as the quantum Hall system (QHS), is responsible for carrying out this comparison. Its working principle consists of submitting each of the two resistors to a known current, and increasing the value of the current I_{H} that circulates in R_{H} until the difference in the voltage drop between the two resistors R_{H} and R_{S} equals zero, measured from a null detector. There is also a fine-tuning of I_{H}, which is done by a QHS subsystem, called superconducting quantum interference device (SQUID). Its operating principle consists of, at temperatures below 4.2 K, increasing I_{H} , if there is any difference between the magnetic fields generated by I_{H} and I_{S} when they flow through coils with N_{H} and N_{S} windings (16 and 2065 turns, respectively). These windings are distinct and electrically isolated (although coupled by a magnetic circuit).

When balance is achieved, one can calculate R_{S} as follows [7]:

$$\frac{R_{\mathrm{S}}}{R_{\mathrm{H}}} = \frac{N_{\mathrm{S}}}{N_{\mathrm{H}}}\left(1 - \frac{I_{\mathrm{B}}}{I_{\mathrm{S}}}\frac{N_{\mathrm{B}}}{N_{\mathrm{S}}}\right), \tag{8}$$

where N_{S} is the number of turns of winding of the coil in series with R_{S}; N_{H} is the number of turns of winding of the coil in series with R_{H}; I_{B} is the current which flows through the coil with N_{B} windings; I_{S} is the current which flows through resistor R_{S}.

3. THE ELECTRIC CURRENT PRIMARY STANDARD BASED ON OHM'S LAW, THE JOSEPHSON EFFECT, AND THE QUANTUM HALL EFFECT

Consider the electric circuit proposed in Figure 8, where the current source is the device under test (DUT), R_{STD} is a resistor that was previously calibrated by the QHS, and V_{STD} is the potential difference across R_{STD}, measured directly by the PJVS system.

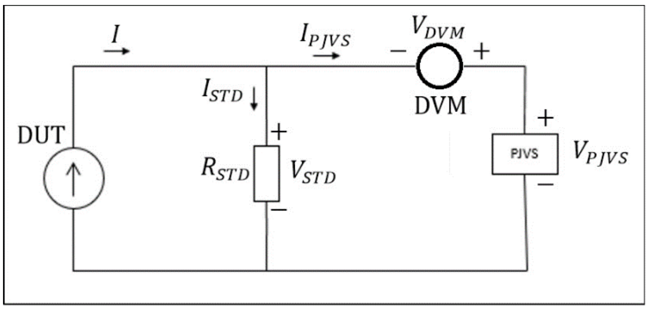

Figure 8. Circuit used to calibrate the current source I from Ohm's law.

One can calculate I_{STD} as follows:

$$I_{\mathrm{STD}} = \frac{V_{\mathrm{STD}}}{R_{\mathrm{STD}}} = \frac{V_{\mathrm{STD}}}{R_0 \times [1 + \alpha \times (T - T_0) + \beta \times (T - T_0)^2]}, \tag{9}$$

where I_{STD} is the current flowing through R_{STD} (the standard resistor); V_{STD} is the voltage measured by the PJVS system; T is the temperature measured by the thermometer; R_0, α, T_0, and β are standard resistor construction parameters.

The I_{PJVS} value is virtually zero, due to the DVM differential connection. Hence, $I = I_{\mathrm{STD}}$. The PJVS system estimates V_{STD} value from V_{PJVS} and V_{DVM} voltages.

Thus, the calibration of the current source I is carried out by comparing the value presented by this current source and the calculated value I_{STD}. The latter is obtained by applying equation (9), which uses V_{STD} values (measured by the PJVS system) and R_{STD} values (informed by the user and with traceability to the QHS system).

To implement this proposal, we used a high-performance Fluke 5730A multifunction calibrator as a device under test (DUT). We also developed a control software in Python, which commands the DUT (through a GPIB interface) to supply the currents to be measured. The user provides the standard resistor value information (R_{STD}) to the software, which gets the V_{STD} value by reading the spreadsheet, where the voltage measurement was recorded by the PJVS system. Therefore, this program estimates the value of the current that flows through R_{STD}, based on the model presented in equation (9), and its associated uncertainty.

The user can register the available standard resistors, as well as the calibrators (the DUT), to be used by the system in the developed software. This allows the software to inform the user of the measurement ranges that can be obtained in the DUT calibration for a selected standard resistor. After the user selects the resistor, the software automatically distributes 5 current measurement points in each range, and if the last range cannot be calibrated at its maximum value, the software automatically distributes 5 points to the maximum possible current for the last range. Additionally, to maintain the integrity of the standard resistor that will be used, the software does not supply the standard resistor with a current greater than the maximum recommended by the resistor manufacturer. It also warns the user of this condition, preventing it from occurring.

4. UNCERTAINTY ANALYSIS

The proposed system mathematical model - equation (9) - allows us to get the standard uncertainty components (for the measurements) presented in Table 1.

Table 1. Summary of standard uncertainty components.

Standard uncertainty component	Source of uncertainty
u_{CSU}	PJVS system
u_{Temp}	Thermometer calibration certificate
u_{resol}	Thermometer resolution
u_{R}	Resistor calibration certificate
u_{A}	Dispersion of the measurements

Figure 9. Setup of the electric current primary standard based on the PJVS and the QHS systems.

u_{CSU} is the PJVS system uncertainty regarding the measurement of the voltage in the standard resistor. u_{Temp} is the uncertainty given by the calibration certificate of the thermometer used to measure the air bath temperature, u_{resol} is the uncertainty related to its resolution, and u_{R} is the uncertainty of the standard resistor (given by the QHS). Such uncertainties are the Type B evaluation of standard uncertainty. u_{A} is the Type A evaluation of standard uncertainty, related to the dispersion of the measurements.

5. RESULTS AND DISCUSSION

In Figure 9, one can see the setup of the electric current primary standard based on the PJVS and the QHS systems. The standard resistors, previously calibrated with the QHS (the latter not shown), are inside the air bath for temperature control (A). A Fluke 5730A calibrator was used as a current source under calibration (the DUT) (B). On the right, there is a rack with the PJVS and the liquid helium cylinder (C). Above the air bath, there is a thermometer, the sensor of which is close to the resistors being calibrated (D). The software described in section 3 is running in the notebook (E). GPIB interfaces are used for communication between the instruments.

Table 2. Lowest and highest relative uncertainties and relative errors by DUT range, for the proposed electric current primary standard based on the PJVS and the QHS systems.

DUT range	Resis-tor	Lowest relative uncert. µA/A	Highest relative uncert. µA/A	Lowest relative error µA/A	Highest relative error µA/A
220 µA (10 µA; 50 µA; 100 µA; 150 µA; 200 µA)	PT20 (10 kΩ)	0.5	1.0	17	18
2.2 mA (0.3 mA; 0.8 mA; 1.2 mA; 1.6 mA; 2.0 mA)	PR06 (100 Ω)	0.7	7.2	100	174
22 mA (2.2 mA; 2.5 mA; 2.6 mA; 2.8 mA; 3.0 mA)	PR06 (100 Ω)	1.5	5.4	137	151
22 mA (3 mA; 4 mA; 6 mA; 8 mA; 10 mA)	PT17 (10 Ω)	2.2	4.6	12	25

Table 3. Some National Metrology Institutes (NMI) best CMC for DC current meter. Expanded uncertainties (k = 2.0) [12].

Country (NMI)	DC current range	Uncertainty range
Brazil (Inmetro)	10 µA to 100 µA	(7.8 to 11) µA/A
	100 µA to 20.0 A	(7.6 to 16) µA/A
EUA (NIST)	10 mA	10 µA/A
France (LNE)	1.0 µA to 100.0 µA	1.3 µA/A
	100 µA to 20.0 A	(1.3 to 8) µA/A
Germany (PTB)	1.0 nA to 100 µA	(3 to 60) µA/A
	100 µA to 10.0 A	3 µA/A

The F5730A was calibrated in DC current from 50 µA to 10 mA. Hence, the ranges calibrated were 200 µA, 2.2 mA, and 22 mA. Considering that the PJVS system is limited to 10 V DC measurements, we decided to use standard resistors of 10 Ω, 100 Ω, and 10 kΩ.

In Table 2, one can see the lowest and highest relative expanded uncertainties ($k = 1.960$ [13]) and relative errors by DUT range. Comparing these preliminary results to the updated best DC current meter CMC (Table 3), it is possible to see that the uncertainties are compatible or even better (Table 2) than the other ones from Table 3. For instance, the proposed system could measure 100 µA with 1.0 µA/A, while in Table 3, such values are between 1.3 µA/A and 3 µA/A.

6. CONCLUSIONS

We proposed an electric current primary standard based on Ohm's law, which is one of the BIPM recommendations to realize the ampere. Preliminary results were presented in the range between nanoampere and milliampere, using two quantum standards: a QHS and a PJVS.

Considering the complexity and costs of using the PJVS and the QHS systems, it is worth using the proposed system, so far, in the range from 50 µA to 10 mA. In this range, the uncertainties are between 0.5 µA/A and 4.6 µA/A, comparable to the best ones in the Calibration and Measurement Capabilities (CMC) acknowledged by the International Bureau of Weights and Measures (BIPM) [11]. This is an ongoing research, and the next goal is to increase the calibration range of the proposed electric current primary standard based on Ohm's law, the Josephson and the quantum Hall effects.

AUTHORS' CONTRIBUTION

Regis P. Landim's contribution to this work was related to conceptualization, investigation, methodology, project administration, resources, supervision, validation, visualization, and writing (original draft, review, and editing).

Wesley C. S. Sousa's contribution to this work was related to data curation, formal analysis, investigation, software, validation, visualization, and writing (original draft).

ACKNOWLEDGEMENT

The authors would like to thank Helio Ricardo Carvalho and Vinicius Coutinho Oliveira, experts in QHS at Inmetro, for the technical information, the calibration of the standard resistors with the QHS, and for allowing the use of Figure 7.

REFERENCES

[1] H. Scherer, D. Drung, C. Krause, Improved calibration of instruments for small direct currents, 2016 Conference on Precision Electromagnetic Measurements (CPEM 2016), Ottawa, ON, Canada, 2016, pp. 1-2.
DOI: 10.1109/CPEM.2016.7540573

[2] F. Liu, C. Liang, Q. He, A data-based approach for online smart meter calibration, Acta IMEKO vol. 9 (2020) no. 2, pp. 32-37.
DOI: 10.21014/acta_imeko.v9i2.777

[3] The BIPM. The International System of Units (SI). 9. ed, 2019. ISBN 978928222720.

[4] T. Van Duzer, C. W. Turner, Principles of Superconductive Devices and Circuits, Prentice Hall PTR, 1998.

[5] Roland H., Reinhold K., Thomas W., Gertrud Z., Review on Superconducting Materials, Applied Superconductivity: Handbook on Devices and Applications, vol. 2 (2016).

[6] S. P. Benz, C. A. Hamilton, Application of the Josephson Effect to Voltage Metrology, In Proceedings of the IEEE, vol. 92 (2004) no. 10, pp. 1617-1629.
DOI: 10.1109/JPROC.2004.833671

[7] R S. M. Ali, Development of Electrical Quantities Primary Standards, Trans. of the Inst. of Measur. and Con., vol 44 (2022), pp. 539-561.
DOI: 10.1177/01423312211030109

[8] N.-H. Kaneko, Review of quantum electrical standards and benefits and effects of the implementation of the “revised SI”, IEEJ Transactions on Electrical and Electronic Engineering, vol. 12 (2017), pp. 627-637
DOI: 10.1002/tee.22492

[9] W. Poirier, F. Schopfer, Resistance metrology based on the quantum Hall effect, Eur. Phys. J. Spec. Top., vol. 172 (2009), p. 207–245.
DOI: 10.1140/epjst/e2009-01051-5

[10] F. Piquemal, G. Genevès, Argument for a Direct Realization of the Quantum Metrological Triangle, Metrol, vol. 37 (2000) no. 3, pp. 207-211
DOI: 10.1088/0026-1394/37/3/4

[11] The BIPM, Mise en pratique for the definition of the ampere and other electric units in the SI - Brochure-Appendix 2, 2019, pp. 3–8. Online [Accessed 25 November 2025]
https://www.bipm.org/utils/en/pdf/si-mep/SI-App2-ampere.pdf

[12] R. Larson, B. Farber, Elementary Statistics: Picturing the World, USA, Prentice Hall, 2008, ISBN 9780132424332.

[13] The BIPM, The CIPM MRA database (KCDB). Online [Accessed 25 November 2025]
https://www.bipm.org/kcdb/